Contents list available at CBIORE journal website

International Journal of Renewable Energy Development

Journal homepage: https://ijred.cbiore.id

Research Article

Characterization of zirconia sulfate catalyst for sustainable aviation fuel from waste cooking oil

Treisnaning Widasgantri[a], Tri Widjaja[a*], Deliana Dahnum[b], Ali Altway[a], Thasya Lamhotmatua[a], Kevin Antonius[a]

[a]*Department of Chemical Engineering, Faculty of Industrial Technology and Systems Engineering, Institut Teknologi Sepuluh Nopember, Jl. Raya ITS, Surabaya, Indonesia*

[b]*Research Center of Chemistry, National Research and Innovation Agency, Tangerang Selatan, Indonesia*

Abstract. The growing accumulation of waste cooking oil (WCO) in Indonesia presents serious environmental concerns while offering potential as a renewable feedstock for sustainable aviation fuel. This study evaluates the conversion of WCO into bio-jet fuel via pyrolytic catalytic cracking (PCC) using cobalt-dispersed sulfated zirconia ($Co/ZrO_2–SO_4$, Co/SZ) catalysts under atmospheric pressure. Sulfated zirconia was synthesized hydrothermally and impregnated with 1, 3, and 5 wt% cobalt. Catalyst characterization by FTIR, XRD, BET, and SEM–EDX confirmed successful cobalt dispersion, preservation of the monoclinic ZrO_2 phase, and increasing surface area with higher cobalt loading (83.93 to 111.19 $m^2 g^{-1}$). Catalytic performance was tested in a fixed-bed reactor at 400, 430, and 460 °C with a feed-to-catalyst ratio of 100:1. GC–MS analysis revealed that both temperature and cobalt loading significantly influenced selectivity toward the jet fuel fraction ($C_{12}–C_{16}$). The highest bio-jet fuel selectivity (68.63%) and yield (57.46 wt%) were obtained using 5 wt% Co/SZ at 400°C. At 430 °C, excessive secondary cracking reduced selectivity to 27.78% for 3 wt% Co/SZ, with gasoline-range products reaching 62.70%. Increasing the temperature to 460 °C partially restored jet-range selectivity to 62.67% for 5 wt% Co/SZ due to enhanced isomerization and aromatization reactions. Reusability tests indicated gradual catalyst deactivation caused by coke deposition and loss of acid sites. These results demonstrate that the synergistic interaction between sulfated zirconia acidity and cobalt's deoxygenation functionality enables efficient WCO conversion into bio-jet fuel, highlighting Co/SZ as a promising catalyst for sustainable aviation fuel production.

Keywords: Waste Cooking Oil, Hydrodeoxygenation, Cobalt-dispersed Sulfated Zirconia Nanocatalyst, Bio-jet Fuel

Received: 8th Dec 2025; Revised: 28th January 2026; Accepted: 15th Feb 2026; Available online: 2nd March 2026

1. Introduction

Currently, the amount of waste cooking oil (WCO) in Indonesia is considerably high. In Java and Bali, restaurants generate approximately 270 kiloliters of WCO annually (Busca, 2007). With the growth of the Indonesian population and the increasing consumption of fried foods, the volume of WCO from households and industries is expected to continue rising. However, every 10 tons of improperly disposed WCO leads to an estimated environmental cleanup cost of IDR 7.2 billion (Garrone *et al.*, 2005). Studies conducted in small to medium-sized restaurants, street vendors, and mobile food sellers reported WCO generation of 18 and 15 liters per day, respectively.

Improper disposal of WCO into the environment, such as directly pouring it into drainage systems, can cause water pollution, pipeline clogging, and the proliferation of pathogenic bacteria (Arata *et al.*, 1990). WCO contains organic matter that increases COD and BOD levels. A thin layer of oil can spread over the water surface, restricting oxygen transfer and significantly reducing dissolved oxygen (DO). This condition favors the growth of anaerobic microorganisms, which often produce foul-smelling gases (Deng *et al.*, 2008). Moreover, fried food residues may contain trace metals that accumulate in the oil. WCO primarily consists of hydrocarbon compounds such as triglycerides, which can be converted into hydrocarbon-based biofuels. However, its high free fatty acid content leads to elevated acidity, potentially causing storage instability and engine corrosion (Reddy *et al.*, 2011).

Waste oils, including WCO, represent valuable feedstocks to produce liquid fuels and value-added chemicals. Converting waste oils into renewable fuels is essential to prevent environmental pollution while generating economic benefits (Wahyono *et al,* 2020). Among various approaches, deoxygenation mechanisms are considered effective for producing high-quality biofuels. Pyrolytic methods are widely recognized as efficient pre-treatment processes for waste oil conversion, offering low production costs (Wu *et al.*, 2010). This method not only removes impurities but also eliminates oxygen atoms to yield hydrocarbons.

The $Co/ZrO_2–SO_4$ catalyst, consisting of sulfated zirconia (SZ) nanoparticles modified with cobalt (Co), exhibits unique structural properties observable via electron microscopy techniques such as SEM and TEM (Zhang *et al.*, 2015). The catalyst is synthesized through wet impregnation, involving cobalt nitrate hexahydrate ($Co(NO_3)_2·6H_2O$) and sulfated

* Corresponding author
Email: tri.widjaja@its.ac.id (T. Widjaja)

https://doi.org/10.61435/ijred.2026.62076
ISSN: 2252-4940/© 2026.The Author(s). Published by CBIORE

zirconia, followed by drying and thermal activation. Application of Co/ZrO_2–SO_4-based catalysts in bio-jet fuel production remains limited, despite their promising potential. WCO, with its high fatty acid content, can be utilized as a sustainable feedstock for the development of green fuels, particularly bio-jet fuel. The production of sustainable bio-jet fuel is gaining global attention as part of efforts to meet future aviation fuel demands and achieve the Net Zero Emissions (NZE) target by 2050 (Fitria *et al*., 2025).

Bio-jet fuel derived from household waste is highly attractive due to its low cost and environmental management benefits (Sekewael *et al*, 2022; Hartati *et al* 2025). It can be produced through several processes, including chemical conversion routes such as transesterification, esterification, and thermal or catalytic cracking. Among these, Pyrolytic Catalytic Cracking (PCC) offers advantages, as it can be carried out under atmospheric pressure and relatively mild temperatures without requiring hydrogen gas, unlike hydrocracking or hydrotreating processes (Xiao *et al*., 2021).

The main challenge addressed in this study is how to effectively utilize WCO as a feedstock for bio-jet fuel production using Co/ZrO_2–SO_4 catalysts. This work also explores strategies for developing Co/ZrO_2–SO_4 catalysts to enhance the conversion of WCO into sustainable aviation fuels while considering infrastructure compatibility and operational costs. The productivity and conversion efficiency achieved from WCO-based bio-jet fuel highlight its potential as a viable alternative fuel pathway for sustainable energy development. To address these three major challenges, an approach has been proposed by utilizing Waste Cooking Oil (WCO) as a feedstock for bio-jet fuel production. This strategy not only minimizes waste and environmental pollution but also avoids competition with edible oil demand, mitigates greenhouse gas effects, and contributes to slowing down global warming. Moreover, it enhances economic value by converting WCO into bio-jet fuel.

The development of Co/ZrO_2–SO_4 catalysts and optimization of the conversion process play an essential role in advancing sustainable bio-jet fuel production. This effort also reduces dependency on imported catalysts, particularly those required for producing environmentally friendly fuels such as bio-jet fuel. The synthesis of Co/ZrO_2–SO_4 catalysts is further improved by employing more efficient solvothermal and hydrothermal techniques, using readily available raw materials. In addition, the high thermal stability of Co/ZrO_2–SO_4 allows its reuse without significant loss of catalytic activity. Consequently, production costs of the catalyst can be reduced while still achieving high-quality bio-jet fuel output.

Previous studies have reported that natural zeolite can be utilized as a catalyst for the hydrodeoxygenation (HDO) process of vegetable oil model compounds, such as lauric acid, into hydrocarbons at 350 °C, achieving a conversion of 52.05%. Another study proposed a strategy for converting waste oils into high-quality products through pyrolysis to investigate the deoxygenation mechanism using a composite catalyst of SAPO-11-Pd/C (Kantcheva *et al*., 2004). Furthermore, K_2O was successfully doped into MgO/CaO catalysts, where the presence of K_2O significantly influenced biofuel production. A reaction temperature of 525 °C was found suitable for catalytic cracking, yielding a high proportion of liquid products (Wako *et al*., 2018).

The novelty of the present study lies in the application of the Co/ZrO_2–SO_4 catalyst, which offers several advantages. Specifically, Co/ZrO_2–SO_4 demonstrates superior catalytic activity in hydrodeoxygenation reactions, the ability to achieve higher liquid product yields with improved selectivity toward bio-jet fuel, and the presence of Brønsted acid sites generated through sulfation, which enhance catalytic performance in hydrocarbon cracking reactions. Process engineering for the optimization of Co/ZrO_2–SO_4 conversion is conducted using Waste Cooking Oil (WCO) as the primary feedstock.

2. Material and methods

2.1 Materials

The materials utilized in this research consist of zirconia nanopowder, cobalt nitrate hexahydrate ($Co(NO_3)_2.6H_2O$), both sourced from CV. Progo Mulyo, deionized water and sulfuric acid supplied by Sumber Ilmiah Persada. The waste cooking oil was obtained from Keputih, Sukolillo, Surabaya.

2.2 Pre-Treatment of Waste Cooking Oil (WCO)

The bleaching process of Waste Cooking Oil (WCO) was performed by adding bleaching earth to the preheated oil. A total of 1 liter of WCO was placed in a heating vessel and heated until reaching hot or near-boiling conditions. Subsequently, 50 g of bleaching earth was gradually added while stirring continuously to ensure homogeneous mixing. Heating was continued until the mixture exhibited a darker color change, after which the process was stopped. The mixture was then allowed to stand for sedimentation. Once the solid phase settled, the clearer upper oil layer was separated from the residue and subsequently used in the cracking process.

2.3 Synthesized of sulfated zirconia

The synthesis of sulfated zirconia (SZ) was carried out using the hydrothermal method. Zirconia powder was mixed with 1.5 M sulfuric acid solution at a ratio of 1:15 (w/v) in an autoclave. The mixture was stirred using a magnetic stirrer for 2 h and subsequently heated in an oven at 120 °C for 4 h. The resulting solid was centrifuged at 2000 rpm for 20 min, followed by drying at 110 °C. The dried material was sieved using a 270-mesh screen and then calcined at 600 °C for 4 h.

2.3 Synthesis of Cobalt-Dispersed Sulfated Zirconia (Co/SZ)

The synthesized sulfated zirconia (SZ) was impregnated with cobalt at different loadings (1%, 3%, and 5% w/w) and dissolved in 20 mL of distilled water. The mixture was stirred for 24 h using a magnetic stirrer. The resulting solid was centrifuged at 2000 rpm for 20 min, dried at 110 °C, and sieved through a 270-mesh screen. The sieved material was subsequently calcined under a nitrogen flow (20 mL/min, 500 °C, 4 h) and further reduced under a hydrogen flow (20 mL/min, 500 °C, 4 h).

2.4 Catalytic performance of the catalysts in bio-jet fuel production

The hydro conversion of waste cooking oil into bio-jet fuel was conducted in a fixed-bed reactor. The working principle of this reactor is that the feed in the furnace is vaporized at a certain temperature. The feed's vapor then hits the catalyst in the reactor, causing the hydrodeoxygenation and/or hydrocracking reaction. The reaction product vapor is the condensed and passes through the condenser to form a liquid product.

Thermal hydro conversion was carried out at various temperatures (400, 430, and 460 ^{0}C) for 2 h, utilizing 300mL of waste cooking oil as the feedstock to identify the optimum reaction temperature. The catalytic performance was evaluated

under these optimum conditions for 2 h, maintaining a feed-to-catalyst ratio of 100:1.

The selectivity of the catalyst during the hydro conversion of waste cooking oil into biofuel is evaluated through GC-MS analysis, which measures the area percentages of the chromatogram corresponding to gasoline fraction (C_5 – C_7), jet fuel fraction (C_{12} – C_{16}), and diesel fraction (>C_{16}). The best bio-jet fuel product was analyzed with FTIR to determine the hydro conversion process and ability to reusable.

3. Result and discussion

3.1 Raw materials analysis

The feedstock used for the synthesis of bio-jet fuel was Waste Cooking Oil (WCO). After physicochemical characterization, the data obtained are presented in Table 1, along with the compositional analysis of WCO determined by GC-MS as shown in Table 2. During repeated frying cycles, WCO undergoes oxidation and polymerization reactions, which increase its molecular weight and viscosity, leading to problems such as foaming and gumming. Furthermore, as shown in Table 1, the relatively high free fatty acid (FFA) and water contents may promote soap formation (Pisarello & Querini, 2013). Therefore, a pre-treatment process was carried out to remove heavy fractions and moisture; these steps significantly reduced the viscosity and improved the oil quality for further conversion processes (Casallas *et al.*, 2018). Based on Table 1, the density and viscosity of WCO decreased after pre-treatment, indicating a reduction in polar compounds and other impurities, although the values remained slightly higher than those specified in SNI 7709:2019 for cooking oil. The FFA content decreased significantly from 4.644% to 0.49% after pre-treatment, demonstrating that the process effectively removed FFAs that could otherwise cause soap formation through saponification reactions and accelerate catalyst deactivation during hydro conversion. This finding is consistent with the study by Yahya (2023), which reported that bleaching earth effectively adsorbs free fatty acids due to its primary component, bentonite, which is rich in montmorillonite with a high specific surface area and active functional groups such as –OH, enabling physical adsorption and electrostatic interactions. Additionally, the reduction in water content from 0.29% to 0.14% is attributed to the hygroscopic nature and high porosity of bleaching earth, allowing it to absorb water molecules trapped within the oil (Abdelbasir *et al.*, 2022). During pre-treatment, bleaching earth was activated by heating at temperatures above 100 °C, facilitating the evaporation of entrapped moisture (Maharani, 2022).

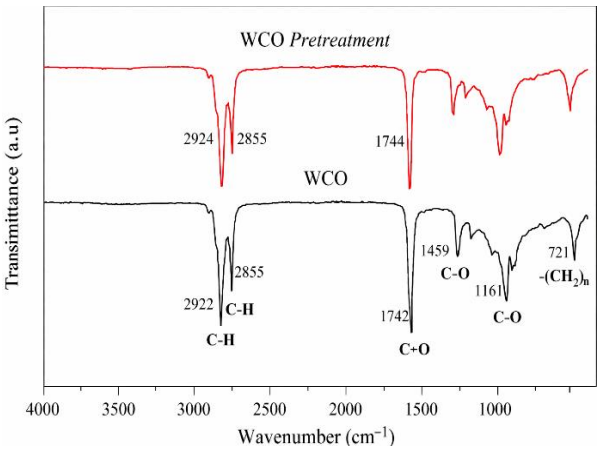

Fig 1 WCO FTIR Spectrum Before and After Pre-treatment

Although the physicochemical properties of WCO changed after pre-treatment, the functional groups of the compounds present did not show significant alterations. This is evidenced by the FTIR analysis of WCO before and after pre-treatment (Figure 1), which indicates no formation or disappearance of functional groups. However, a decrease in the absorption intensity of −(CH_2)n, C–O, and C–H bonds at wavenumbers of 721, 1744, and 2853–2924 cm^{-1} was observed after pre-treatment. This weakening suggests a reduction in long-chain carbon compounds, likely originating from organic impurities.

The GC–MS results presented in Table 2 show that WCO is predominantly composed of oleic acid and linoleic acid, along with other fatty acid components. These fatty acids serve as key precursors in hydrocarbon fuel synthesis because their long carbon chains (C16–C18) can be converted into fuel fractions within the C8–C16 range through cracking and hydroisomerization processes (Atabani *et al.*, 2013).

Table 1
Characteristic of Waste Cooking Oil

Physicochemical Features @25 ºC	Cooking Oil (SNI 7709:2019)	WCO Before Pre-Treatment	WCO After Pre-Treatment
Density (g/cm^3)	0.89	0.91	0.908
Viscosity Kinematics (mm^2/s)	43.6	46.217	44.053
FFA (%)	Max. 0.3	4.644	0.497
Water Content (%)	Max. 0.1	0.29	0.14

Table 2
Main Components of WCO GC-MS Results

Components	Area (%)	Chemical Formula
Oleic *acid*	33.83	$C_{18}H_{34}O_2$
Linoleic *acid*	32.64	$C_{18}H_{32}O_2$
Palmitic *acid*	9.84	$C_{16}H_{32}O_2$
Omega-3 *fatty acid*	9.35	$C_{18}H_{30}O_2$
Stearic *acid*	4.44	$C_{18}H_{36}O_2$
Myristic *acid*	0.24	$C_{14}H_{28}O_2$
Omega-9 *fatty acid*	0.49	$C_{20}H_{38}O_2$
Others	9.35	

3.2 FT-IR Analysis of Cobalt-Dispersed Sulfated Zirconia (Co/SZ) Catalysts

Fourier Transform Infrared (FT-IR) analysis was conducted to identify the functional groups present in the synthesized materials. The spectra are shown in Figure 2 within the wavenumber range of 650–4000 cm^{-1}. For the 1% cobalt concentration, characteristic peaks were observed at 3337.8, 3458.97, 3524.20, and 3572.65 cm^{-1}. At 3% cobalt concentration, peaks appeared at 3369.5, 3403.9, 3486.9, 3505.6, 3527.9, 3550.3, and 3570.8 cm^{-1}. Meanwhile, for 5% cobalt loading, the detected peaks were located at 3488.8, 3507.4, 3529.8, 3550.3, 3570.8, and 3591.3 cm^{-1}. The peak distribution in the 3200–3600 cm^{-1} range corresponds to multiple –OH stretching vibrations, indicating the presence of hydrated surfaces or abundant hydroxyl sites (Busca, 2007; Prameswari *et al* 2023). The variations in both the number and position of peaks among the samples suggest that cobalt impregnation influences the –OH environment (through hydrogen bonding or substitution by Co) (Garrone *et al*., 2005). This is significant, as the interaction between Co and –OH groups may alter the acidity and adsorption properties of the catalyst (Garrone *et al*., 2005).

Typically, sulfate vibrations (asymmetric SO_4^{2-}) are observed within 1200–1000 cm^{-1}, while SO_4^{2-} bending vibrations occur in the 600–700 cm^{-1} region. However, in the obtained FT-IR data, no distinct peaks were recorded within 650–2000 cm^{-1}. This absence implies that sulfate-related bands may not have been extracted in the spectra, although they are theoretically expected in Co–SZ. Additionally, dispersed cobalt species are known to form Co–O bonds, generally characterized by absorption in the 500–700 cm^{-1} range. The available spectra predominantly displayed –OH bands, suggesting that Co–O and sulfate vibrations may not have been clearly resolved.

Nevertheless, characteristic sulfate absorption bands were identified between 1046–1248 cm^{-1}, confirming the presence of covalent coordination between SO_4^{2-} groups and Zr^{4+} ions on the zirconia surface (Deng *et al*., 2008). The bands at approximately 1100–1230 cm^{-1} correspond to asymmetric S–O stretching vibrations, while those around 1050 cm^{-1} are associated with symmetric stretching modes (Wu *et al*., 2010). Furthermore, absorption at 1630 cm^{-1} and in the 3300–3500 cm^{-1} range indicates O–H vibrations, originating from chemically bound and physically adsorbed water molecules on the catalyst surface (Wu *et al*., 2010).

The comparison of band intensities reveals that increasing cobalt concentration reduces the intensity of SO_4^{2-} bands, indicating cobalt dispersion on the SZ surface without altering the fundamental ZrO_2 structure (Zhang *et al*., 2015). This finding is consistent with previous reports, which state that the incorporation of transition metals such as cobalt affects sulfate dispersion through interactions with active surface sites, thereby contributing to enhanced catalytic activity (Fitria *et al*, 2024).

3.3 BET Analysis of Co/SZ Catalysts

The Brunauer–Emmett–Teller (BET) technique was employed to evaluate the specific surface area, pore volume, and pore diameter of the synthesized catalysts. The BET analysis was conducted at the Integrated Laboratory of UPN Veteran Jawa Timur. The results are presented in Table 3. The data in Table 3 show the physicochemical properties of Co/SZ catalysts obtained from N_2 physisorption analysis. The Co-1/SZ catalyst exhibited a specific surface area of 83.929 $m^2\ g^{-1}$, which increased to 94.135 $m^2\ g^{-1}$ and 111.192 $m^2\ g^{-1}$ for Co-3/SZ and Co-5/SZ, respectively. This increase in specific surface area indicates that cobalt effectively enhances the textural properties of the SZ catalysts (Fitria *et al,* 2025).

The improvement in surface area at higher cobalt concentrations can be attributed to the role of cobalt in generating additional active sites through its 3d orbitals containing unpaired electrons (Fitria *et al,* 2025). These unpaired electrons exhibit strong affinity toward adsorbates, thereby promoting N_2 adsorption on the catalyst surface and contributing to the overall increase in the calculated specific surface area (Fitria *et al,* 2025).

3.4 XRD Analysis of Co/SZ Catalysts

X-ray Diffraction (XRD) analysis was performed to determine the crystallinity of the synthesized Co/SZ catalysts. The diffraction patterns, shown in Figure 3, were recorded

Table 3
BET Analysis Results of Co/SZ Catalyst

Catalyst	Specific Surface Area (SA_{BET}) (m^2g^{-1})	Pore Diameter (D_{pore}) (nm)
Co-1/SZ	83.929	32.495
Co-3/SZ	94.135	28.972
C0-5/SZ	111.192	24.528

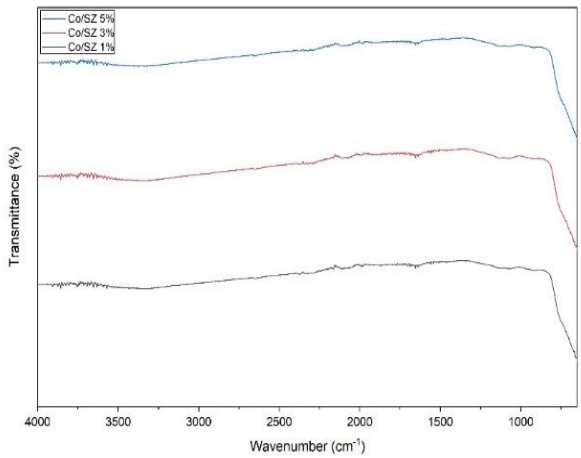

Fig 2 FT-IR Spectra Results of Co/SZ Catalyst Synthesis

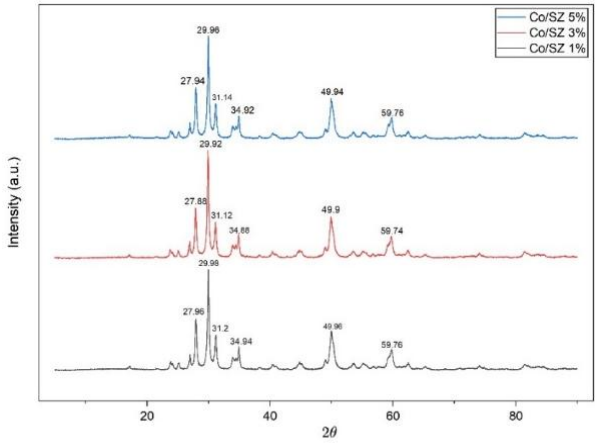

Fig 3 XRD Curve of Co/SZ Catalyst

within a 2θ range of 5°–90°. According to the JCPDS reference card No. 37-1484, the diffraction peaks correspond to the monoclinic crystalline phase of ZrO_2. The diffraction patterns indicated that all samples exhibited monoclinic ZrO_2 phases without any phase transitions (Fitria *et al*, 2025). This finding suggests that both sulfation and cobalt dispersion at different concentrations did not alter the primary crystalline phase of ZrO_2 (Fitria *et al*, 2025).

As shown in Figure 3, the XRD patterns of Co/SZ catalysts with cobalt loadings of 1%, 3%, and 5% displayed main diffraction peaks at approximately 27.9°, 29.9°, 31.1°, 34.9°, 49.9°, and 59.7°, consistent with the monoclinic ZrO_2 phase (JCPDS No. 37-1484). The peak intensities increased with higher cobalt concentrations, particularly at 3% and 5%, indicating enhanced crystallinity or lattice ordering due to cobalt dispersion on the SZ surface. This phenomenon is consistent with reports that transition metals such as cobalt may act as promoters to stabilize crystal structures and mitigate amorphization effects caused by sulfation (Sekewael *et al*, 2022).

Nevertheless, at higher cobalt loading (5%), minor phases of Co_3O_4 may potentially appear, although the diffraction patterns remained predominantly characterized by ZrO_2 peaks (Kantcheva *et al.*, 2004). Overall, the results indicate that cobalt concentration influences the intensity and sharpness of XRD peaks, reflecting changes in crystallinity and crystallite size. These structural modifications may subsequently affect the density and stability of acid-metal active sites, which are crucial for catalytic performance.

3.5 SEM-EDX Analysis of Co/SZ Catalyst

Scanning Electron Microscope (SEM) analysis aims to examine the morphology of the synthesized Co/SZ catalyst, while EDX is used to determine the elemental composition in specific areas of the Co/SZ catalyst. The analysis was conducted at the Department of Mechanical Engineering ITS using a 20K magnification. The morphology of the synthesized Co/SZ catalyst can be seen in Figure 4, while the elemental composition of SZ, Co-1/SZ, Co-3/SZ, and Co-5/SZ is shown in Table 4.

Based on Figure 4 (a), it can be observed that the unsaturated sulfate zirconia catalyst has dense particles with relatively uniform particle size. The structure tends to have very small pores, and the particle shape is predominantly pseudo-spherical. This is consistent with literature, indicating that sulfate zirconia calcined at high temperatures tends to form tight aggregates with limited surface area (Garcia-Sancho *et al.*, 2018). Figure 4 (b) shows that the addition of 1% cobalt leads to significant texture changes. There is a noticeable presence of smaller and more dispersed aggregates compared to pure sulfate zirconia samples. The surface appears rougher with fine deposits, which are suspected to be cobalt oxide (Co_3O_4) particles dispersed on the ZrO2 surface. The more homogeneous particle distribution suggests that impregnation at low concentrations results in good dispersion without excessive agglomeration. Figure 4 (c) shows that the addition of 3% cobalt leads to the tendency of cobalt particle agglomeration. Small clusters or nodules (around 50-100 nm) are deposited on the surface or between ZrO2 particles. The basic ZrO2 structure is still visible, but the pores between particles appear to be more closed by the cobalt deposit. This indicates that at medium concentrations, cobalt metal begins to form a secondary phase that could affect the surface area and accessibility of active sites (Shan *et al.*, 2018). Impregnation of 5% cobalt, as seen in Figure 4 (d), results in a more heterogeneous morphology with larger aggregates and clearer deposit layers. There is a tendency for pore blocking by cobalt particles, which could reduce the effective surface area of the catalyst. However, the cobalt deposits are still uniformly

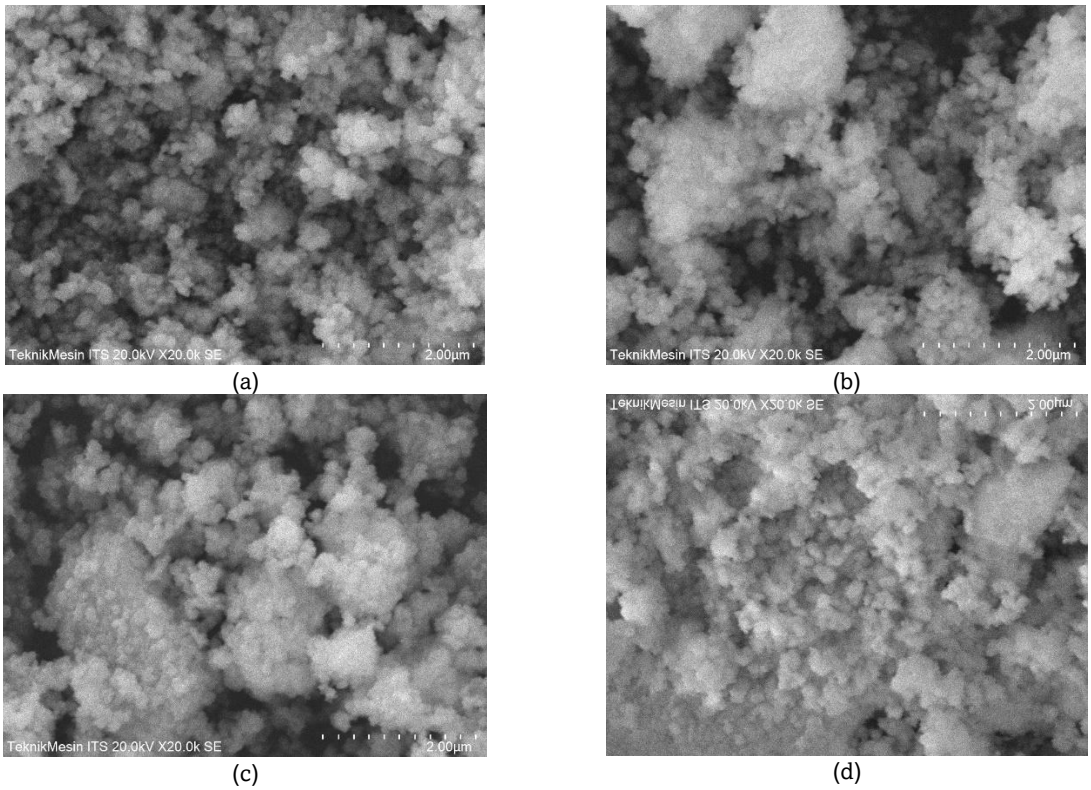

Fig 4 SEM results (a) SZ, (b) Co-1/SZ, (c) Co-3/SZ, (d) Co-5/SZ

Table 4
Elemental composition of Co/SZ catalysts analyzed by EDX

Sample	Elemental Composition (wt%)			
	Zr	O	S	Co
SZ	70.94	29.06	nd	nd
Co-1/SZ	72.54	25.83	nd	1.64
Co-3/SZ	65.24	33.70	nd	1.06
Co-5/SZ	68.39	30.31	nd	1.29

nd = not detected

distributed across the surface without forming separate phases. Catalysts with good metal dispersion tend to have higher activity due to the greater exposure of active sites (Zhao *et al*., 2020).

Based on Table 4, zirconia contains only zirconium and oxygen. The cobalt content in Co-1/SZ, Co-3/SZ, and Co-5/SZ shows successful cobalt dispersion on SZ with uniform distribution. Sulphur (S) was not detected in all samples, indicating that sulphur likely vanished during the calcination process or was below the EDX detection limit. This is common for sulphate catalysts that undergo thermal decomposition (Yamaguchi, 1990). Cobalt (Co) was successfully detected in the impregnated samples. This indicates that Co is dispersed on the ZrO2 surface, although it may not be fully detected due to matrix effects or uneven distribution. Homogeneous Co distribution is important to ensure that catalytic active sites are evenly available. Agglomeration can reduce the active surface area and negatively affect catalytic activity (Shan *et al*., 2018). The addition of Co causes a gradual decrease in the Zr percentage in accordance with the metal addition to the matrix. Additionally, the addition of Co leads to an increased O/Zr ratio in the 3% and 5% Co samples. This indicates the presence of oxygen from Co_3O_4 or Co-O-Zr interactions, which may enhance the oxidative properties of the catalyst.

ZrO_2-SO_4 catalysts are known as superacid solids active in isomerization, alkylation, and esterification reactions (Hino *et al*., 1980). The addition of cobalt is expected to enhance redox activity, such as in oxidation or hydrogenation reactions (Zhao *et al*., 2020).

3.6 Production of Bio-Jet Fuel from Waste Cooking Oil (WCO) via Pyrolytic Catalytic Cracking (PCC)

Following catalyst characterization, the catalyst performance in the Pyrolytic Catalytic Cracking (PCC) process was evaluated to determine its catalytic activity and selectivity in converting Waste Cooking Oil (WCO) into bio-jet fuel. The cracking process was conducted using fixed-bed reactor equipped with a tray fitted with a mesh screen (100 mesh) serving as the catalyst holder.

During the PCC process, both thermal cracking and catalytic reactions occurred. High cracking temperatures were applied to ensure that the feedstock (WCO) underwent phase transformation into the gas phase and interacted effectively with the catalyst, thereby promoting hydro conversion reactions, including hydrodeoxygenation and/or hydrocracking. The resulting products were subsequently condensed through a condenser to form an Oil Liquid Product (OLP).

A previous investigation by Fitria *et al* (2025) reported that the highest OLP yield during the hydro conversion of Palm Cooking Oil (PCO) without a catalyst, conducted for 2 hours within a temperature range of 400–550 °C, was obtained at 450 °C. In contrast, at higher temperatures of 500 °C and 550 °C, the products were predominantly in the gas phase (Fitria *et al,* 2025). Based on Table 1, the characteristics of pre-treated WCO closely resemble those of cooking oil in accordance with the Indonesian National Standard SNI 7709:2019. Therefore, the optimal temperature conditions previously identified for PCO were considered applicable to pre-treated WCO. Consequently, the cracking temperatures selected for this study were 400 °C, 430 °C, and 460 °C to determine the most optimal operating temperature.

The PCC process is influenced not only by operating temperature but also by reaction time, heating rate, catalyst type, catalyst-to-feed ratio, and impregnated metal concentration (Wako *et al*., 2018). Accordingly, this study also investigates the effects of catalyst type and metal impregnation concentration. The catalyst used in this study was Co/SZ (sulphated zirconia impregnated with cobalt metal). Cobalt impregnation was selected based on previous studies, particularly Gupta *et al.* (2023), which reported that cobalt is a transition metal with strong catalytic properties and is highly effective in activating hydrogen molecules (H_2) through homolytic dissociation of the H–H bond, facilitated by unpaired electrons in its 3d orbitals. In addition, cobalt exhibits excellent catalytic activity due to its ability to interact with Lewis's acid sites associated with its vacant 4p orbitals, enabling more efficient interactions with feed molecules. Cobalt is capable of cleaving C–O bonds during hydrodeoxygenation reactions, thereby removing oxygen from fatty acid molecules and producing more stable hydrocarbons with lower oxygen content (Kumar *et al*., 2019).

The metal impregnation concentrations were varied at 1%, 3%, and 5%, with relatively wide intervals between variables to better identify the optimal impregnation condition. Regarding reaction time and heating rate, identical conditions were applied in all experiments, namely no fixed reaction time limit, with the reaction terminated when no further OLP formation was observed, and a constant heating rate was maintained. Furthermore, the catalyst-to-feed ratio used in this study was 1:100 (w/v) relative to 100 mL of WCO, following the optimal condition (Fitria *et al*, 2025). The resulting OLP was subsequently analysed using Gas Chromatography–Mass Spectrometry (GC–MS) to identify the chemical composition of the liquid products and to determine the distribution of hydrocarbon fractions formed, which served as the basis for evaluating catalyst selectivity.

3.7 Effect of Reaction Temperature on Selectivity over Co/SZ Catalyst

Based on GC–MS analysis as shown in Figure 5, at a reaction temperature of 400 °C, all Co/SZ catalysts exhibited high bio-jet fuel selectivity, with values of 61.46% for Co–SZ 1%, 58.68% for Co–SZ 3%, and 68.63% for Co–SZ 5%. These results indicate that 400 °C represents an optimal condition for deoxygenation and cracking processes to obtain the bio-jet fuel fraction.

Based on Figure 5, when the temperature was increased to 430 °C, a decrease in bio-jet fuel selectivity was observed for all Co/SZ catalysts, particularly for Co–SZ 3%, which dropped sharply to 27.78%. Meanwhile, Co–SZ 1% and Co–SZ 5% maintained relatively high selectivity values of 62.58% and

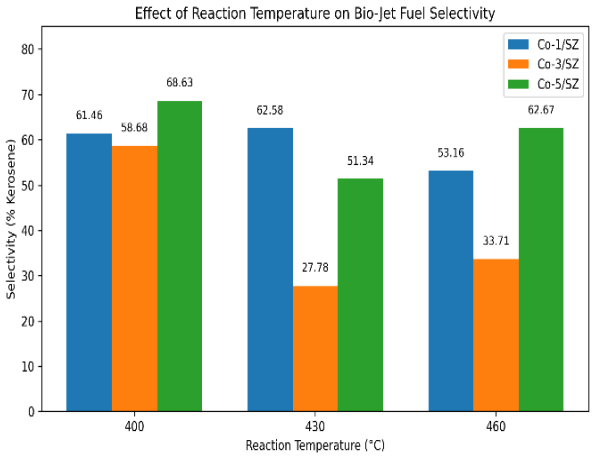

Fig 5 Effect of Reaction Temperature on Bio-jet Fuel Selectivity over Co/SZ Catalyst

51.34%, respectively. This decline suggests that secondary cracking occurred at intermediate temperatures, leading to the conversion of part of the bio-jet fuel fraction into bio gasoline with shorter carbon-chain lengths.

A further increase in temperature to 460 °C resulted in different trends, where bio-jet fuel selectivity increased again for Co/SZ 5% to 62.67%, while Co/SZ 1% decreased to 53.16% and Co/SZ 3% increased to 33.71%. Overall, these results indicate the occurrence of isomerization and aromatization processes, which promote the formation of stable aromatic rings within the bio-jet fuel fraction. This contributes to enhanced thermal stability of the catalyst and helps maintain the carbon-chain range characteristic of bio-jet fuel even at elevated temperatures (Sirajuddin, 2013).

3.8 Effect of Cobalt Impregnation Loading and Temperature on Bio-jet Fuel Selectivity

Based on the data presented in Figure 6 (a), at an operating temperature of 400°C, the bio-jet fuel selectivity increases linearly with increasing Co loading on the catalyst, rising from 61.46% to 68.63% at 5% Co/SZ. This behaviour indicates that higher metal loading increases the number of available active sites, thereby enhancing the deoxygenation of triglycerides through decarboxylation and decarbonylation pathways. The increased Co content strengthens the catalyst's ability to selectively cleave C–O bonds, promoting the formation of medium-chain hydrocarbons (C_{12}–C_{16}), which constitute the main components of bio-jet fuel.

At an operating temperature of 430 °C, as shown in Figure 6(b), an anomalous trend is observed in which the bio-jet fuel selectivity sharply decreases to 27.78% at 3% Co/SZ, followed by a recovery to 51.34% at 5% Co/SZ. From a mechanistic perspective, the elevated temperature combined with intermediate metal loading (3%) intensifies secondary cracking reactions, resulting in a significant shift of products toward the bio gasoline range (C_5–C_{11}), reaching 62.70%. However, at a higher Co loading of 5%, the substantially increased number of metal sites provides a more pronounced hydrogenation function. This effect moderates excessive chain scission, allowing radical intermediates to be rapidly saturated into medium-chain alkanes before undergoing further cracking into lighter fractions.

At 460 °C, as illustrated in Figure 6 (c), the bio-jet fuel selectivity initially decreases to 53.16% but subsequently

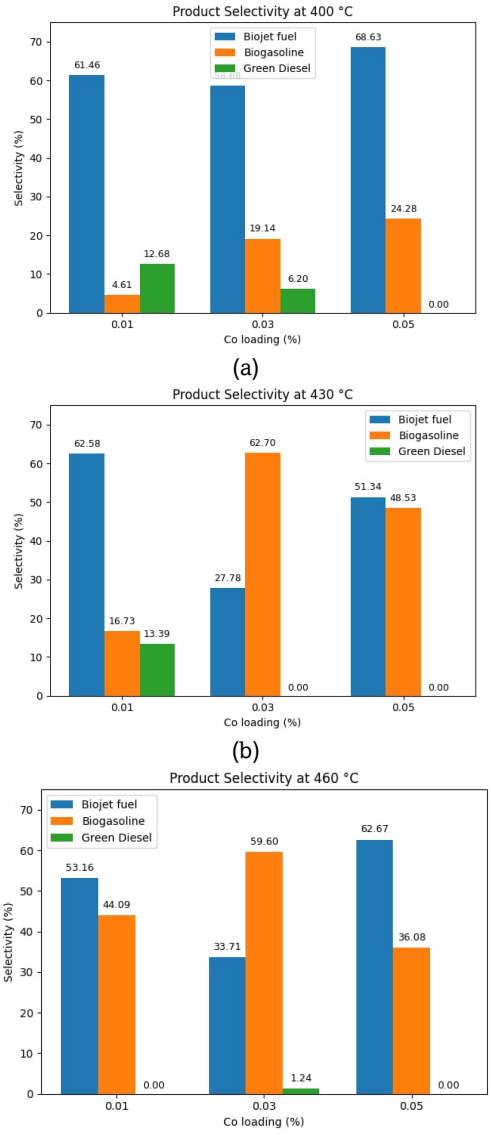

Fig 6 Effect of Co loading (%) on the selectivity toward bio-jet fuel, bio gasoline, and green diesel at (a) 400 °C, (b) 430 °C, and (c) 460 °C

increases markedly to 62.67% with increasing Co loading up to 5%. At this elevated temperature, catalytic activity tends to decline due to catalyst deactivation, which suppresses exce ssive cracking reactions and redirects the product distribution toward longer-chain hydrocarbons, favouring the formation of bio-jet fuel (Sekewael *et al*, 2022).

3.9 Effect of Operating Condition Variations on Bio-jet Fuel Yield

Following the recapitulation of GC-MS data and subsequent yield calculations, the selectivity and yield of bio-jet fuel produced from waste cooking oil (WCO) over Co/SZ catalysts with metal impregnation loadings of 1%, 3%, and 5% are summarized in Table 5.

As shown in Table 5, variations in reaction temperature and cobalt impregnation loading significantly affect the bio-jet fuel yield. In this study, a heterogeneous catalytic system was employed, in which the catalyst consists of two main components: an active metal dopant and a support material (carrier) (Sekewael *et al*, 2022). The uniform dispersion of cobalt

Table 5
Selectivity and Yield of Bio-jet Fuel

Catalysts	Temperature (ºC)	Selectivity (%)	*Yield* (%wt)
Co/SZ 1%	400	61.46	53.01
	430	62.58	58.74
	460	53.16	55.84
Co/SZ 3%	400	58.68	55.94
	430	27.78	51.38
	460	33.71	51.90
Co/SZ 5%	400	68.63	57.46
	430	51.34	52.93
	460	62.67	56.08

metal on the acidic sulphated zirconia support, combined with its relatively high surface area, helps suppress catalyst sintering during the reaction.

The primary objective of this study is to evaluate the performance of Co/SZ catalysts in converting WCO into bio-jet fuel. Among the investigated conditions, the highest bio-jet fuel yield of 57.46 wt% was achieved using the 5% Co/SZ catalyst at a reaction temperature of 400 °C.

3.10 Catalyst reusability analysis

The FTIR spectra of the oil liquid product (OLP) obtained from the pyrolytic catalytic cracking of waste cooking oil (WCO) over cobalt impregnated sulfated zirconia (Co/SZ) catalyst exhibit significant variations across catalyst reuse cycles (fresh use, reuse 1, reuse 2), as shown in Figure 7. Considering that WCO predominantly consists of triglycerides and free fatty acids (C16–C18), its catalytic transformation into bio-jet fuel involves complex reactions, including thermal cracking, β-scission, decarboxylation, decarbonylation, isomerization, and aromatization pathways (Bridgwater, 2012; Kubicka *et al.*, 2010; Corma *et al.*, 2007). Therefore, the evolution of functional groups observed in the FTIR spectra provides important insight into the catalytic performance and stability during repeated use.

In the fresh catalyst condition based on Figure 7, strong absorption bands are observed in the range of 2950–2850 cm^{-1}, corresponding to asymmetric and symmetric stretching vibrations of aliphatic C–H bonds (–CH_3 and –CH_2– groups). These bands indicate the dominance of saturated and partially saturated hydrocarbons, which are characteristic of jet fuel-range fractions (C_8–C_{16}). Conventional aviation fuels mainly consist of n-alkanes, iso-alkanes, cycloalkanes, and limited aromatics within this carbon range (Speight, 2014). The pronounced intensity of these bands in the fresh catalyst suggests that Co/SZ effectively promotes C–C bond cleavage of long-chain fatty acids through strong Brønsted acid sites associated with sulphated zirconia (Hino *et al.*, 1980). However, a noticeable reduction in intensity is observed in reuse 1, and the bands become significantly weakened in reuse 2, indicating a substantial decline in hydrocarbon production within the jet fuel range. This trend reflects progressive catalyst deactivation during repeated cycles.

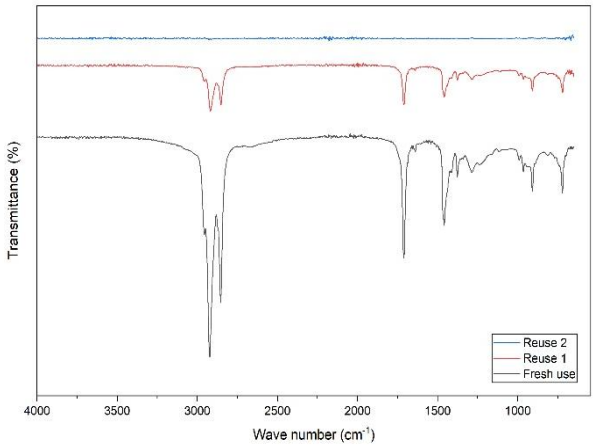

Fig 7 FTIR Spectra of Catalyst Reuse Cycles

A distinct absorption band around 1700–1740 cm^{-1}, corresponding to C=O stretching vibrations of carbonyl groups, is clearly present in the fresh catalyst sample. These carbonyl species may originate from residual esters, ketones formed during secondary cracking reactions, or unconverted fatty acids. In bio-jet fuel production, the removal of oxygen is crucial, as oxygenated compounds reduce heating value, increase acidity, and compromise thermal stability (Kubicka *et al.*, 2010). Deoxygenation pathways such as decarboxylation and decarbonylation are expected to reduce the carbonyl content (Kubicka *et al.*, 2010; Bejblova *et al.*, 2009). Although the intensity of the C=O band decreases in reuse 1 and reuse 2, this reduction is more plausibly attributed to the overall decline in liquid product yield rather than improved deoxygenation efficiency. The weakened signal in reuse 2 suggests diminished catalytic conversion rather than enhanced product quality.

The band observed near 1600 cm^{-1} in the fresh catalyst corresponds to C=C stretching vibrations of aromatic structures. Aromatic hydrocarbons can form through oligomerization and cyclization of olefinic intermediates promoted by strong acid sites (Corma, 1995). In aviation fuels, a controlled number of aromatics is required for elastomer seal compatibility; however, excessive aromatic content may increase soot formation during combustion. The clear presence of aromatic signals in the fresh catalyst indicates that Co/SZ possesses sufficient acidity to facilitate mild aromatization reactions. Nevertheless, the significant attenuation of this band in reuse 2 indicates the loss of active acid sites responsible for these transformations.

The spectral region between 1200 and 1000 cm^{-1}, associated with C–O stretching vibrations of esters, alcohols, and ethers, also shows decreasing intensity with increasing reuse cycles. These oxygen-containing functionalities are typically derived from partially converted triglycerides or intermediate oxygenates formed during pyrolysis (Bridgwater, 2012). The substantial reduction of these bands in reuse 2 again reflects a lower extent of catalytic conversion and reduced formation of liquid oxygenated intermediates.

The pronounced decrease in overall peak intensities observed in reuse 2 strongly suggests catalyst deactivation. Sulphated zirconia is recognized as a superacid catalyst with high cracking activity but is also susceptible to coke deposition under high-temperature hydrocarbon processing conditions (Hino *et al.*, 1980; Yamaguchi, 1994). Coke formation may occur via polymerization of olefinic intermediates and condensation of aromatic species, leading to blockage of Brønsted and Lewis acid sites. Additionally, the sulphate groups (SO_4^{2-}), which are responsible for the super acidity of zirconia, can undergo thermal degradation or leaching during repeated reaction cycles, resulting in a significant reduction in total acidity (Yamaguchi, 1994). Furthermore, cobalt species that promote deoxygenation and hydrogen-transfer reactions may experience agglomeration or sintering, reducing their redox functionality and further limiting catalytic efficiency (Corma *et al.*, 2007).

Overall, the FTIR analysis demonstrates that the fresh Co/SZ catalyst effectively converts WCO into hydrocarbon-rich liquid products compatible with the jet fuel range, as evidenced by dominant aliphatic C–H vibrations and moderate aromatic formation. However, catalyst reusability without regeneration leads to progressive deactivation, characterized by diminished hydrocarbon formation and reduced overall liquid yield. The loss of super acidity due to sulphate degradation, coke deposition, and potential cobalt sintering collectively contributes to the observed decline in catalytic performance. These findings highlight the necessity of catalyst regeneration strategies or structural modification to enhance long-term stability for sustainable bio-aviation fuel production.

3.11 By-Products

Following the catalytic cracking process, the products obtained consist not only of the oil liquid product (OLP) as the main product but also include residual solids and coke. To evaluate whether the PCC process proceeded optimally, FTIR analysis was conducted to identify the chemical characteristics of the generated residue.

Based on the FTIR analysis shown in Figure 8, several absorption bands were identified, indicating the presence of heavy hydrocarbons and oxygenated compounds that were not fully converted during the reaction. The formation of residue suggests that not all heavy WCO molecules were successfully converted into lighter fractions, primarily due to diffusion limitations of large molecules toward the active sites of the catalyst (Corma, 1994). The absorption bands observed at approximately 2922 cm^{-1} and 2853 cm^{-1} correspond to asymmetric and symmetric stretching vibrations of aliphatic C–H bonds in methylene ($–CH_2–$) and methyl ($–CH_3$) groups, which are characteristic of long-chain hydrocarbons (Guillen *et al*., 2004; Muik *et al*, 2007). The presence of these bands indicates that a fraction of heavy WCO molecules retained their aliphatic structures and did not undergo complete C–C bond cleavage.

A strong absorption band at 1746 cm^{-1} is attributed to the stretching vibration of the carbonyl (–C=O) group, indicating the presence of ester functionalities. Carbonyl groups are characteristic structures of WCO, which is rich in triglycerides and free fatty acids, as summarized in Table 1 and Table 2.

Another absorption band observed at 1459 cm^{-1} corresponds to the bending vibration of –C–H bonds in methylene groups ($–CH_2–$), further confirming that long-chain hydrocarbons constitute the dominant components of the residue. Additionally, an absorption band at 1159 cm^{-1} is assigned to the stretching vibration of –C–O bonds, indicating the presence of oxygenated compounds as partial products or reaction intermediates formed during the cracking process (Rohman *et al*., 2010).

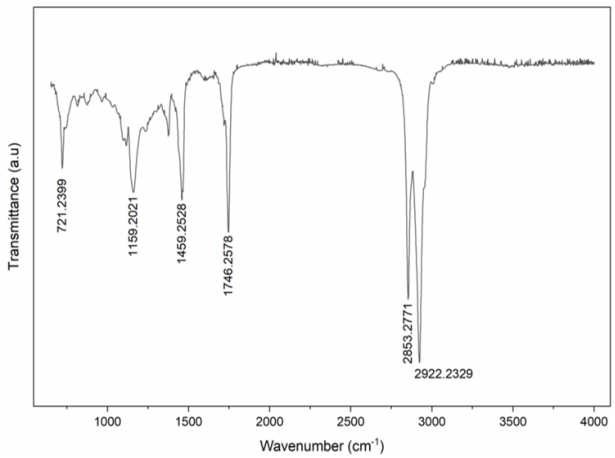

Fig 8 FTIR Spectra of the PCC Residue

The absorption band at 721 cm^{-1} is associated with the rocking vibration of $–(CH_2)_n–$ groups, which is a distinctive feature of linear long-chain hydrocarbons. The presence of this band suggests the formation of heavy fractions or wax-like compounds, which may originate from secondary condensation and polymerization reactions occurring during the PCC process (Ragunathan *et al*., 2020). Therefore, the FTIR results of the residue confirm that the formation of waxy residues is a consequence of incomplete cracking and the predominance of secondary reactions, which can ultimately reduce the selectivity toward light liquid products (OLP) and potentially contribute to coke formation on the catalyst surface during the PCC process.

4. Conclusion

This study demonstrates the successful conversion of waste cooking oil (WCO) into bio-jet fuel using cobalt-dispersed sulfated zirconia ($Co/ZrO_2–SO_4$, Co/SZ) catalysts through a pyrolytic catalytic cracking (PCC) process under atmospheric pressure and relatively mild operating conditions. The physicochemical characterization results confirmed that cobalt impregnation significantly influenced the structural, textural, and acidic properties of the sulfated zirconia support. FTIR analysis verified the presence of sulfate groups and surface hydroxyls, while XRD results showed that the monoclinic ZrO_2 phase was preserved after cobalt incorporation. BET analysis revealed that increasing cobalt loading enhanced the specific surface area, and SEM–EDX confirmed the successful dispersion of cobalt on the catalyst surface.

Catalytic performance evaluation indicated that both reaction temperature and cobalt impregnation loading strongly affected bio-jet fuel selectivity and yield. Among the investigated conditions, the 5% Co/SZ catalyst exhibited the best performance, achieving the highest bio-jet fuel selectivity of 68.63% and the maximum yield of 57.46 wt% at 400 °C. This performance is attributed to the synergistic effect between the strong Brønsted acidity of sulfated zirconia and the hydrogenation–deoxygenation functionality provided by cobalt, which promotes selective C–O bond cleavage and favors the formation of medium-chain hydrocarbons ($C_{12}–C_{16}$) characteristic of bio-jet fuel.

At higher temperatures, secondary cracking reactions became more pronounced, leading to increased formation of lighter hydrocarbon fractions and by-products. FTIR analysis of the PCC residue confirmed the presence of long-chain hydrocarbons, ester groups, and oxygenated compounds, indicating incomplete cracking and the occurrence of secondary condensation and polymerization reactions, which may contribute to waxy residue and coke formation.

Overall, the results highlight the potential of Co/SZ catalysts as effective and economical catalysts for sustainable aviation fuel production from waste-derived feedstocks. The utilization of WCO not only addresses environmental concerns related to waste disposal but also offers a promising pathway for producing renewable bio-jet fuel. Future studies should focus on catalyst stability, regeneration performance, and scale-up considerations to further enhance the feasibility of this process for industrial applications.

Acknowledgments

The author would like to thank all colleagues who have provided much support in completing the research and writing

this article. The research was conducted as an activity at Industrial Waste Processing Laboratory.

Author Contributions: **Treisnaning Widasgantri**: Conceptualization, methodology, formal analysis, writing—original draft, **Tri Widjaja**; supervision, resources, project administration, **Deliana Dahnum**; supervision, resources, project administration, **Ali Altway**; supervision, resources, project administration, **Thasya Lamhotmatua**; writing—review and editing, project administration, validation, **Kevin Antonius**; writing—review and editing, project administration, validation. All authors have read and agreed to the published version of the manuscript.

Funding: This research was funded by the Ministry of Higher Education, Science and Technology Indonesia through BIMA *Penelitian Tesis Magister*.

Conflicts of Interest: The authors declare no conflict of interest.

References

Abdelbasir, S. M., Hassan, S. S. M., Kamel, A. H., & El-Nasr, R. S. (2022). Waste cooking oil recycling for biodiesel production: Improvement of oil quality using adsorption techniques. *Fuel, 309*, 122156. https://doi.org/10.1016/j.fuel.2021.122156

Arata, K., & Hino, M. (1990). Preparation and catalytic properties of solid superacids of sulfated metal oxides. *Applied Catalysis, 59*, 197–204. https://doi.org/10.1016/0254-0584(90)90012-Y

Atabani, A. E., Silitonga, A. S., Badruddin, I. A., Mahlia, T. M. I., Masjuki, H. H., & Mekhilef, S. (2013). A comprehensive review on biodiesel as an alternative energy resource and its characteristics. *Renewable and Sustainable Energy Reviews, 16(4), 2070–2093.* https://doi.org/10.1016/j.rser.2012.10.037

Banchapattanasakda, W., Asavatesanupap, C., & Santikunaporn, M. (2023). Conversion of waste cooking oil into bio-fuel via pyrolysis using activated carbon as a catalyst. *Molecules, 28*, 3590. https://doi.org/10.3390/molecules28093590

Bridgwater, A. V. (2012). Review of fast pyrolysis of biomass and product upgrading. *Renewable and Sustainable Energy Reviews, 16*(3), 1969–1985. https://doi.org/10.1016/j.rser.2011.12.016

Busca, G. (2007). Acid–base characterization of solid catalysts. *Catalysis Today, 41*, 191–206. https://doi.org/10.1016/S0920-5861(98)00049-2

Casallas, D., Morales, G., & Pérez, A. (2018). Pretreatment of waste cooking oil for biodiesel production using low-cost adsorbents. *Journal of Environmental Chemical Engineering, 6*(6), 7067–7074. https://doi.org/10.1016/j.jece.2018.10.049

Corma, A. (1995). Inorganic solid acids and their use in acid-catalyzed hydrocarbon reactions. *Chemical Reviews, 95*(3), 559–614. https://doi.org/10.1021/cr00035a006

Corma, A., Huber, G. W., Sauvanaud, L., & O'Connor, P. (2007). Processing biomass-derived oxygenates in the oil refinery: Catalytic cracking (FCC) reaction pathways and role of catalyst. *Journal of Catalysis, 247*(2), 307–327. https://doi.org/10.1016/j.jcat.2007.01.023

Deng, Y., Wang, Y., Liu, X., Zhang, Z., & Guo, Y. (2008). *Journal of Molecular Catalysis A: Chemical,* 279(2), 219–225. https://doi.org/10.1016/j.molcata.2007.10.017

Fitria, R. A., Prasetyo, N., Saviola, A. J., Trisunaryanti, W., Syoufian, A., Amin, A. K., Oh, W.-C., & Wijaya, K. (2025). Synthesis of cobalt-dispersed sulfated zirconia nanocatalyst for the hydroconversion of used palm cooking oil into bio-jet fuel. *Case Studies in Chemical and Environmental Engineering, 11*, 101052. https://doi.org/10.1016/j.cscee.2024.101052

García-Sancho, C., Moreno-Tost, R., Mérida-Robles, J., Santamaría-González, J., & Maireles-Torres, P. (2018). Influence of the sulfation method on the activity of ZrO_2–SO_4^{2-} catalysts. *Catalysis Today, 304*, 34–41. https://doi.org/10.1016/j.cattod.2017.10.020

Garrone, E., & Otero Areán, C. (2005). Variable temperature FTIR spectroscopy of OH groups in zeolites. *Chemical Society Reviews, 34*, 846–857. https://doi.org/10.1039/B406964E

Guillén, M. D., Cabo, N., Ibargoitia, M. L., & Ruiz, A. (2004). Study of the oxidative stability of oils by FTIR spectroscopy. *Journal of the Science of Food and Agriculture*, 84(12), 1521-1531. https://doi.org/10.1002/jsfa.1824

Gupta, A. K. (2023). Recent advances in transition metal-based catalysts for hydrodeoxygenation of bio-oil and waste-derived feedstocks. *Fuel*. https://doi.org/10.1016/j.fuel.2023.128308

Hartati, H., Firda, P. B. D., Prasetyoko, D., Anggoro, D. D., Bahruji, H., Sakti, S. C. W., Holilah, H., & Nugraha, R. E. (2025). Conversion of volcano mud and marble waste to Ni/Ca/ZSM-5 catalyst for bio-jet fuel production from waste cooking oil and the effect of Ni loading. *Fuel*, *400*, Article 135756. https://doi.org/10.1016/j.fuel.2025.135756

Hino, M., & Arata, K. (1980). Solid catalyst treated with anion. 2. Reactions of butane and isobutane catalyzed by zirconium oxide treated with sulfate ion. *Journal of the Chemical Society, Chemical Communications*, 851–852. https://doi.org/10.1039/C39800000851

Kantcheva, M., Hadjiivanov, K., & Klissurski, D. (2004). Cobalt supported on zirconia and sulfated zirconia I: FT-IR and XRD study. *Journal of Catalysis*, 221(1), 1-14. https://doi.org/10.1016/j.jcat.2003.08.019

Kubička, D., & Kaluža, L. (2010). Deoxygenation of vegetable oils over sulfided Ni, Mo and NiMo catalysts. *Applied Catalysis A: General, 372*(2), 199–208. https://doi.org/10.1016/j.apcata.2009.10.034

Kubička, D., Bejblová, M., & Vlk, J. (2009). Conversion of vegetable oils into hydrocarbons over CoMo/MCM-41 catalysts. *Topics in Catalysis, 52*, 161–168. https://doi.org/10.1007/s11244-008-9168-3

Kumar, A., Sharma, S., & Dixit, S. (2019). Data interpretation and applications in structure elucidation and analysis of small molecules and nanostructures. In S.K. Sharma (Ed.), *Advanced Spectroscopic Techniques* (pp. 77–96). Academic Press. https://doi.org/10.1016/B978-0-12-814802-8.00003-3

Muik, B., Lendl, B., Molina-Díaz, A., & Ayora-Cañada, M. J. (2007). Direct monitoring of lipid oxidation in edible oils by Fourier transform infrared spectroscopy. *Chemistry and Physics of Lipids*, 148(1), 34-33. https://doi.org/10.1016/j.chemphyslip.2007.03.004

Pisarello, M. L., & Querini, C. A. (2013). Esterification of free fatty acids using niobium oxide as catalyst in biodiesel production. *Energy Conversion and Management, 70*, 161–166. https://doi.org/10.1016/j.enconman.2013.02.018

Prameswari, J., Widayat, W., Buchori, L., Hadiyanto, H. (2023). Novel iron sand-derived α-Fe2O3/CaO2 bifunctional catalyst for waste cooking oil-based biodiesel production. *Environmental Science and Pollution Research,* 30 (44), 98832 - 98847. https://doi.org/10.1007/s11356-022-21942-z

Ragunathan, B., Kumar, P. S., & Rajendran, S. (2020). Catalytic cracking of waste cooking oil for hydrocarbon fuel production: A review. *Renewable and Sustainable Energy Reviews*, 119, 109550. https://doi.org/10.1016/j.rser.2019.109550

Reddy, B. M., Reddy, E. P., & Lakshmanan, P. (2011). Sulfated zirconia as an efficient solid acid catalyst for organic transformations. *Catalysis Today, 160*(1), 3–10. https://doi.org/10.1016/j.cattod.2010.09.026

Rohman, A., Che Man, Y. B., Ismail, A., & Hashim, P. (2010). The use of Fourier transform infrared (FTIR) spectroscopy in the detection and quantification of adulteration in virgin coconut oil. *Food Chemistry, 129*(2), 583–588. https://doi.org/10.1016/j.foodchem.2011.04.070

Sekewael, S. J., Pratika, R. A., Hauli, L., Amin, A. K., Utami, M., & Wijaya, K. (2022). Recent Progress on Sulfated Nanozirconia as a Solid Acid Catalyst in the Hydrocracking Reaction. *Catalysts*, *12*(2), 191. https://doi.org/10.3390/catal12020191

Shan, W., Luo, M., Ying, P., Shen, W., & Li, C. (2018). The role of cobalt in Co–ZrO_2 catalysts for Fischer–Tropsch synthesis. *Catalysis Today, 299*, 58–67. https://doi.org/10.1016/j.cattod.2017.07.025

Sirajuddin, M. K. (2013). Thermal cracking and isomerization behavior of long-chain hydrocarbons in biofuel production. *Energy Conversion and Management*, 42–49. https://doi.org/10.1016/j.enconman.2013.05.024

Speight, J. G. (2014). *The chemistry and technology of petroleum* (5th ed.). CRC Press.

Wahyono, Y., Hadiyanto, H., Budihardjo, M.A., Adiansyah, J.S. (2020). Assessing the environmental performance of palm oil biodiesel production in indonesia: A life cycle assessment approach. *Energies*, 13 (12), 3248. https://doi.org/10.3390/en13123248

Wako, F. M., Reshad, A. S., Bhalerao, M. S., & Goud, V. V. (2018). Catalytic cracking of waste cooking oil for biofuel production using zirconium oxide catalyst. *Industrial Crops & Products*, 118, 282-289. https://doi.org/10.1016/j.indcrop.2018.03.047

Wu, S., Shu, Q., & Zhang, Q. (2010). Catalytic performance of sulfated zirconia in biodiesel production. *Applied Catalysis B: Environmental, 96*(1–2), 101–109. https://doi.org/10.1016/j.apcatb.2010.02.016

Xiao, T., Wang, X., Liang, C., Zhang, J., & Wang, Y. (2021). Phase tuning of ZrO_2 supported cobalt catalysts for hydrodeoxygenation of 5-hydroxymethylfurfural to 2,5-dimethylfuran under mild conditions. *Applied Catalysis A: General, 623*, 118283. https://doi.org/10.1016/j.apcata.2021.118283

Yamaguchi, T. (1990). Recent progress in solid superacid. *Applied Catalysis, 61*(1), 1–25. https://doi.org/10.1016/S0166-9834(00)82532-5

Yamaguchi, T. (1994). Application of ZrO_2 as a catalyst and a catalyst support. *Catalysis Today, 20*(2), 199–218. https://doi.org/10.1016/0920-5861(94)80194-3

Zhang, Y., Li, H., Liu, Y., Zhao, X., & Wang, G. (2015). Structural and acidic properties of sulfated zirconia catalysts prepared by different methods. *Microporous and Mesoporous Materials, 214*, 1–8. https://doi.org/10.1016/j.micromeso.2015.04.003

Zhao, Y., Li, S., Sun, Y., & Wang, G. (2020). Cobalt-modified zirconia-based catalysts for catalytic oxidation of volatile organic compounds. *Chemical Engineering Journal, 381*, 122693. https://doi.org/10.1016/j.cej.2019.122693